Pion electromagnetic form factor in the covariant spectator theory

Elmar P. Biernat,[1,*] Franz Gross,[2,†] M. T. Peña,[1,‡] and Alfred Stadler[3,§]

[1]*Centro de Física Teórica de Partículas (CFTP), Instituto Superior Técnico (IST),*
Universidade de Lisboa, Avenida Rovisco Pais, 1049-001 Lisboa, Portugal
[2]*Thomas Jefferson National Accelerator Facility (JLab), Newport News, Virginia 23606, USA*
[3]*Departamento de Física da Universidade de Évora, 7000-671 Évora, Portugal*
and Centro de Física Nuclear da Universidade de Lisboa (CFNUL), 1649-003 Lisboa, Portugal

The pion electromagnetic form factor at spacelike momentum transfer is calculated in relativistic impulse approximation using the covariant spectator theory. The same dressed quark mass function and the equation for the pion bound-state vertex function as discussed in the companion paper are used for the calculation, together with a dressed quark current that satisfies the Ward-Takahashi identity. The results obtained for the pion form factor are in agreement with experimental data, they exhibit the typical monopole behavior at high-momentum transfer, and they satisfy some remarkable scaling relations.

I. INTRODUCTION

In the companion paper, Ref. [1], a model for the $q\bar{q}$ interaction was developed that uses the Nambu-Jona-Lasinio mechanism to ensure that a pion bound state of zero mass exists whenever mass can be spontaneously generated through the self-interactions that dress a massless quark. A novel feature of this model is its simplicity; in momentum space, the kernel is the sum of a pure vector δ-function interaction and an interaction which provides confinement, so that even though a feature of the covariant spectator theory (CST) [2–4] is that one of the quarks can be on shell (where both the q and $\bar{q}$ will sometimes be referred to collectively as "quarks"), both quarks in the pair can never be on shell simultaneously. The confining interaction can be a mixture of vector and scalar exchanges, but in the chiral limit (where the undressed mass of the quark, m_0, is zero) the scalar part of the confining interaction decouples, allowing the chirally invariant vector interactions to preserve the features of chiral symmetry. In Ref. [1], the mass function was calculated by fitting two model parameters to lattice data, and the bound-state $q\bar{q}$ equations were defined and their properties studied.

It is the purpose of this paper to show that the simple model introduced and fixed in Ref. [1] can be used to calculate the pion form factor without modifications. This is the first demonstration showing how the model can be applied to a variety of interesting physics problems. Even though the CST has been well studied and used in previous calculations of nuclear form factors [5,6], this calculation introduces a number of new issues never before encountered. The discussion here will not only lead to some interesting new results, but also extend understanding of how to

use the CST. Discussion of the results, and comparison with some previous work, is saved for the last section.

II. PION FORM FACTOR IN THE BETHE-SALPETER THEORY

The electromagnetic pion form factor in the spacelike region has been calculated in a great variety of different approaches; see, e.g., Refs. [7–19]. We begin by reviewing the discussion of the pion form factor in the Bethe-Salpeter (BS) formalism. We will consider a positively charged π^+ consisting of a u and a $\bar{d}$ quark; the form factor for the π^- can be obtained by charge conjugation. In impulse approximation, the electromagnetic form factor of the π^+ is extracted from the sum of two triangle diagrams, in which the photon couples either to the u or the $\bar{d}$ quark, as depicted in Fig. 1.

The top diagram, with the $\bar{d}$ quark as spectator, is weighted by the u quark's electric charge $\frac{2}{3}$ e, while the bottom diagram, with the u quark as spectator, is weighted by the electric charge $-\frac{1}{3}$ e of the d quark traveling backward in time. The sum of the two diagrams is

$$
\begin{aligned}
J^\mu(P_+, P_-) &= \mathrm{e} F_\pi(Q^2)(P_+ + P_-)^\mu \\
&= \frac{2}{3}\,\mathrm{e}\int\frac{\mathrm{d}^4 k}{(2\pi)^4}\,\mathrm{tr}[\bar{\Gamma}_{\mathrm{BS}}(k, p_+) \\
&\quad \times S(p_+)j^\mu(p_+, p_-)S(p_-)\Gamma_{\mathrm{BS}}(p_-, k)S(k)] \\
&\quad - \frac{1}{3}\,\mathrm{e}\int\frac{\mathrm{d}^4 k}{(2\pi)^4}\,\mathrm{tr}[\Gamma_{\mathrm{BS}}(k, p'_-) \\
&\quad \times S(p'_-)j^\mu(p'_-, p'_+)S(p'_+)\bar{\Gamma}_{\mathrm{BS}}(p'_+, k)S(k)],
\end{aligned}
\tag{1}
$$

where $p_\pm = k + P_\pm$, $p'_\pm = k - P_\pm$, $j^\mu(p_+, p_-)$ is the dressed current for off-shell quarks (defined below), and $S(p)$ is the dressed propagator of a quark with momentum p:

*elmar.biernat@tecnico.ulisboa.pt
†gross@jlab.org
‡teresa.pena@tecnico.ulisboa.pt
§stadler@uevora.pt

$$S(p) = Z(p^2) \frac{M(p^2) + \not{p}}{M^2(p^2) - p^2 - i\epsilon}, \qquad (2)$$

with $M(p^2)$ being the quark mass function and $Z(p^2)$ the wave function renormalization, as discussed in Ref. [1] and reviewed below. For the model considered here, $Z(p^2) = 1$. The quark mass function $M(p^2)$ is obtained from the solution of the CST Dyson equation for the self-energy, and the constituent (dressed) mass m of the quark is then determined from the condition $M(m^2) = m$. We assume equal masses for the u and d quarks, so the u and d propagators are identical. Finally, following the notation of Ref. [1], the vertex function $\Gamma_{\mathrm{BS}}(p_1, p_2)$ describes a π^+ coupling to an *outgoing u* quark of momentum p_1 and an *incoming d* quark of momentum p_2 (the same as an *outgoing $\bar{d}$* quark of momentum $-p_2$), while $\bar{\Gamma}_{\mathrm{BS}}(p_1, p_2)$ describes a π^+ coupling to an *incoming u* quark of momentum p_1 and an *outgoing d* quark of momentum p_2 (the same as an *incoming $\bar{d}$* quark of momentum $-p_2$).

Before turning to the CST formalism, we show how the second contribution to the form factor can be transformed into the first, and the two added together. To do this, we need the following transformations of the vertex function and the current under charge conjugation:

$$\mathcal{C}\Gamma_{\mathrm{BS}}^{\mathsf{T}}(p_1, p_2)\mathcal{C}^{-1} = \Gamma_{\mathrm{BS}}(-p_2, -p_1),$$
$$\mathcal{C}j^{\mu\mathsf{T}}(p', p)\mathcal{C}^{-1} = -j^\mu(-p, -p'). \qquad (3)$$

While these relations can be derived from general principles, they also follow from the typical matrix structure of Γ_{BS} [such as $\Gamma_{\mathrm{BS}}(p_1, p_2) \sim (m - \not{p}_1)\gamma^5(m - \not{p}_2)$] or j^μ [such as $j^\mu(p', p) \sim (m - \not{p}')\gamma^\mu(m - \not{p})$]. Taking the transpose of the trace, inserting $\mathcal{C}\mathcal{C}^{-1} = 1$ between the operators, and using the properties in Eq. (3) converts the trace from the second term of Eq. (1) into

$$\mathrm{tr}[\cdots] \rightarrow -\mathrm{tr}[\bar{\Gamma}_{\mathrm{BS}}(-k, -p'_+)S(-p'_+)j^\mu(-p'_+, -p'_-)$$
$$\times S(-p'_-)\Gamma_{\mathrm{BS}}(-p'_-, -k)S(-k)]. \qquad (4)$$

Now, changing $k \rightarrow -k$ under the integral and noting that this converts $p'_\pm \rightarrow -p_\pm$ shows that the trace in Eq. (4) is identical to the trace in the first term of Eq. (1), except for the minus sign which converts the factor $-\frac{1}{3} \rightarrow \frac{1}{3}$. Hence, the two terms are identical (except for the charges), and their sum equals the first term with the factor of $\frac{2}{3}\mathrm{e}$ replaced by e. Note that the ability to change $k \rightarrow -k$ under the integral was essential to the argument.

This discussion can be easily extended to show that the π^0 form factor is identically zero, and that except for a sign, the π^- form factor is identical to the π^+ form factor.

III. PION FORM FACTOR IN THE CST

In the CST, the integral over the relative momentum of the two propagating particles is constrained by the requirement that one of the two particles must always be on shell,

with contributions from terms when both particles are off shell moved to higher order in the series of terms that define the relativistic two-body kernel. The motivation for this rearrangement of terms is that, in many examples, it can be shown that the off-shell terms (from box diagrams, for example) tend to cancel other higher-order terms in the kernel (crossed box diagrams, for example), so that keeping one particle on shell not only simplifies the equations but also improves the convergence of the approximation to the underlying field theory.

The pion form factor in CST will therefore also involve triangle diagrams similar to the BS diagrams shown in Fig. 1, but with the internal particles constrained to their mass shell in the same way that they are constrained in the two-body bound-state equation. As shown in Ref. [1], a careful treatment of the pion bound state in the chiral limit requires a four-channel equation, with contributions from the positive and negative energy poles of both particles included. The full treatment of the triangle diagram for the π^+ form factor using the four-channel equation would therefore involve contributions from the positive- and negative-energy poles of both the u and $\bar{d}$ quarks.

In this first calculation of the pion form factor using CST, we chose to make some approximations that still preserve the
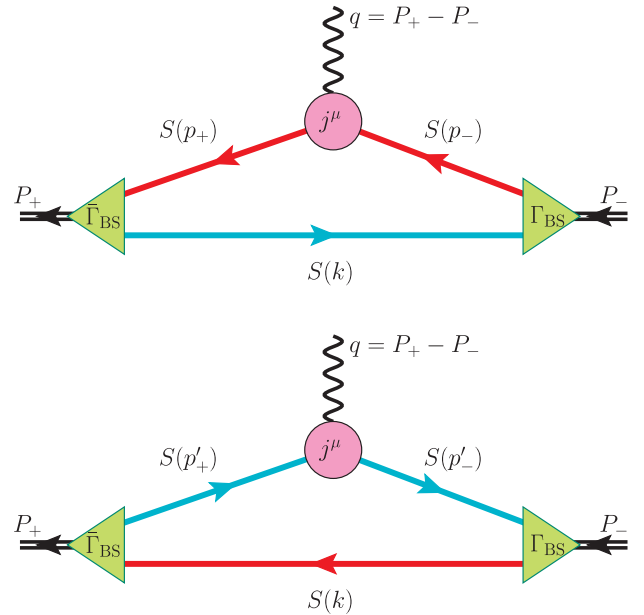

FIG. 1 (color online). The two triangle diagrams for the electromagnetic pion form factor. Here $P_\pm$ are the outgoing and incoming (on-shell) pion four-momenta, q is the four-momentum of the virtual photon, S is the dressed quark propagator, Γ_{BS} is the Bethe-Salpeter pion vertex function, and j^μ is the electromagnetic off-shell quark current. The top diagram describes the interaction of the virtual photon with the u quark, with the $\bar{d}$ quark (represented by a d quark traveling backward in time with momentum k) as a spectator; the bottom diagram represents the interaction of the virtual photon with the $\bar{d}$ quark (again represented by a d quark traveling backward in time), with the u quark as the spectator.

important physics. To understand these approximations, study the location of the particle poles in the BS diagrams of Eq. (1) and Fig. 1. First, concentrate on the diagram where the photon couples to the u quark, and the $\bar{d}$ quark is spectator (top panel in Fig. 1). This diagram has six propagator poles in the complex k_0 plane, three of them in the lower and three in the upper half plane [20]. In the Breit frame, where

$$P_\pm = \left\{ P_0, \mathbf{0}, \pm \frac{1}{2} Q \right\}, \qquad q = \{0, \mathbf{0}, Q\}, \qquad (5)$$

with $P_0 = \sqrt{\mu^2 + \frac{1}{4}Q^2}$, μ the pion mass, and Q the photon momentum transfer, the poles of the spectator d quark are located at $k_0 = \pm E_k \mp i\epsilon$, denoted $1^\pm$, where $E_k = (m^2 + \mathbf{k}^2)^{1/2}$, and the poles of the struck u quark with momenta p_- and p_+ are at

$$k_0 = -P_0 \pm \sqrt{m^2 + \mathbf{k}_\perp^2 + \left(k_z - \frac{Q}{2} \right)^2} \mp i\epsilon,$$

$$k_0 = -P_0 \pm \sqrt{m^2 + \mathbf{k}_\perp^2 + \left(k_z + \frac{Q}{2} \right)^2} \mp i\epsilon, \qquad (6)$$

denoted $2^\pm$ and $3^\pm$, respectively. Since the square roots in the last two expressions are positive, recalling that $p_\pm = k + P_\pm$ means that 2^+ and 3^+ are the positive-energy poles and 2^- and 3^- are the negative-energy poles of the struck u quark. The locations of these six poles in the complex k_0 plane depend on m, μ, Q, k_z and $\mathbf{k}_\perp = (k_x, k_y)$, and are shown in Fig. 2 for two different pion masses.

Before proceeding further, recall that the masses in the denominators of the propagators are not fixed, but are functions of the four-momenta, so that, for example, the denominator of the spectator propagator is $M^2(k^2) - k^2$, not $m^2 - k^2$. *At the pole*, however, the mass condition $M(m^2) = m$ holds, so that the location and movement of the poles can be computed just as if the masses were fixed.

The full four-channel CST equation requires averaging the contributions from all of the propagator poles in the upper and lower half planes. Study of the bottom panel of Fig. 2 shows that when μ is comparable to the dressed quark mass m, the largest contribution will come from the 1^- pole. For small Q (and small $|\mathbf{k}|$), it is close to the poles at 2^+ and 3^+ in the lower half plane, and at the same time far away from the other poles. This is the on-shell contribution of the spectator, with the physical energy of the outgoing $\bar{d}$ antiquark in its *positive*-energy state (because the incoming d quark is in its *negative* energy state). This approximation, used previously in the study of deuteron form factors, is known as the relativistic impulse approximation (RIA) [21–24].

The top panel of Fig. 2 shows that for small μ (and also small Q), all of the poles in the upper half plane are close to each other (and will coalesce into a triple pole when both $Q = 0$ and $\mu = 0$). The requirement that the limit $\mu \to 0$ be described correctly is precisely what led to the need for a
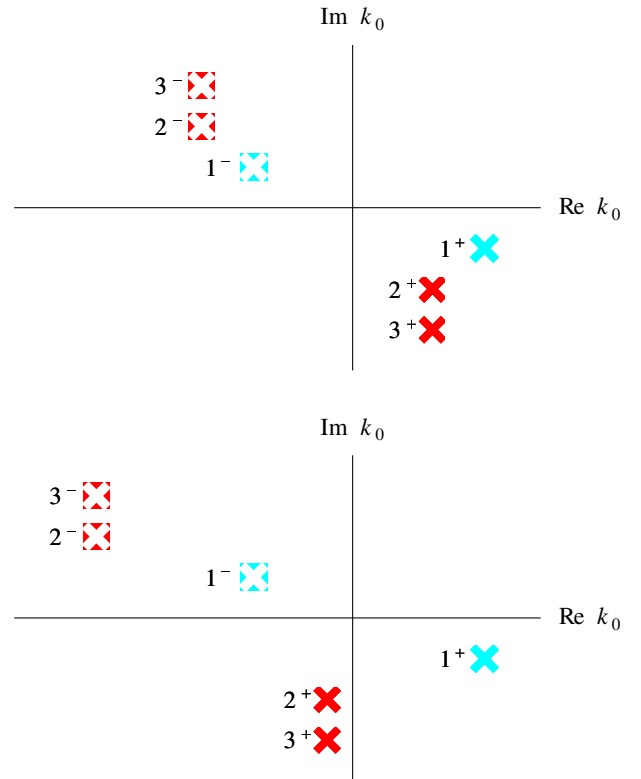

FIG. 2 (color online). The locations of the six propagator poles in the complex k_0 plane of the diagram where the d quark is spectator, shown here for both Q and $|\mathbf{k}|$ small, with $m = 0.308$ GeV. The top panel shows the case when $\mu = 0.14$ GeV; the bottom shows the case when $\mu = 0.42$ GeV. Note that large and different imaginary parts ϵ have been chosen for each pole in order to spread them out in the complex plane for better illustration, but in all cases $\epsilon \to 0$ is implied.

four-channel CST equation in the first place, and these additional channels, included in contributions from the 2^- and 3^- poles, are also needed for a correct description of the form factor in the limit when *both* μ and Q are small.

In this first calculation, we will use the RIA, and hence we cannot expect to be able to correctly describe the form factor in the limit when both μ and Q are small, where the neglected contributions from the 2^- and 3^- poles cannot be ignored (in fact, the RIA becomes singular when both Q and μ tend to zero).

The case when Q is large poses an interesting issue. In this case the position of the poles is quite insensitive to the value of μ, and therefore the RIA describes the form factor equally well for both large and small μ. However, as $k_z \to Q/2$, the integrand becomes large, with the precise role of the poles depending on whether or not k_z is less than or greater than $Q/2$ [recall Eq. (6)]. If $k_z \lesssim Q/2$, the poles 1^- and 2^+ pinch, as shown in the top panel of Fig. 3, while if $k_z \gtrsim Q/2$, the poles 1^- and 2^- are close together, as illustrated in the bottom panel of Fig. 3. In both cases it looks like the integral could be singular, but it remains finite (and small). Briefly, to see what is happening, it
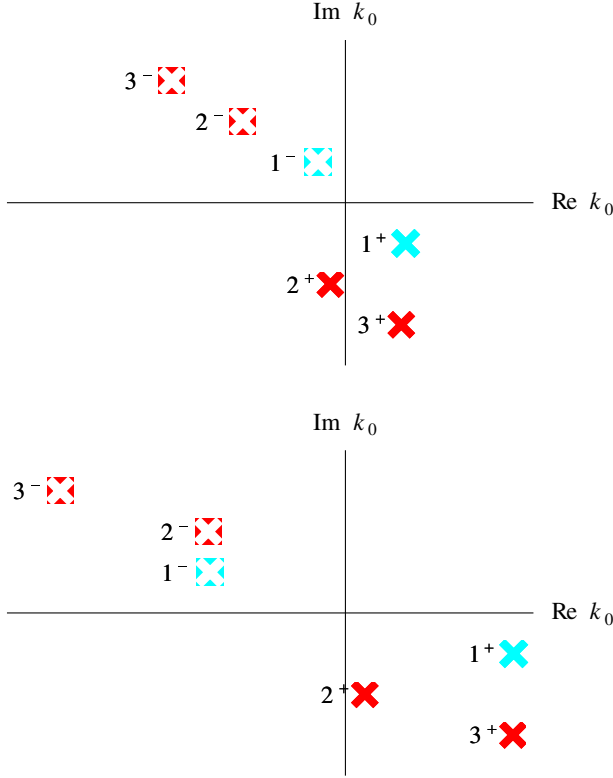
FIG. 3 (color online). The locations of the same six propagator poles shown in Fig. 2, with $m = 0.308$ GeV, $\mu = 0.14$ GeV, and $k_\perp = 0$, but with Q large. The top panel shows the case when $k_z \lesssim Q/2$ and the poles 1^- and 2^+ pinch; the lower panel shows the case when $k_z \gtrsim Q/2$ and the poles 1^- and 2^- get close to each other.

is necessary to examine the behavior of the propagator with momentum p_- when the residue of the pole 1^- is evaluated, i.e., when the spectator is on its negative-energy mass shell, with $k_0 = -E_k + i\epsilon$. The relevant integral is

$$I \sim \int dk_z f(k_z)[m^2 - p_-^2]^{-1}$$
$$= \int dk_z f(k_z)[-\mu^2 + 2P_0 E_k - Qk_z]^{-1}, \qquad (7)$$

where we have approximated $M^2(p_-^2) \simeq m^2$, because we are interested in the kinematics where p_-^2 is close to m^2, and $f(k_z)$ is the remainder of the integrand which provides the needed convergence when $k_z \to \infty$. As Q becomes very large, this integral peaks at very large k_z but is still finite. To estimate it, we expand the factors

$$\lim_{Q\to\infty} I \to \int dk_z \frac{f(k_z)}{Qk_z}\left[\left(1 + \frac{2\mu^2}{Q^2}\right)\left(1 + \frac{E_\perp^2}{2k_z^2}\right) - 1\right]^{-1}$$
$$\simeq \int dk_z f(k_z)\left[\frac{2\mu^2 k_z}{Q} + \frac{E_\perp^2 Q}{2k_z} - \mu^2\right]^{-1}, \qquad (8)$$

where $E_\perp = \sqrt{m^2 + k_\perp^2}$. This shows that the integrand peaks at $k_z = E_\perp Q/(2\mu)$, and it is finite there provided

that $\mu < 2m$. Because the peak is located at large values of k_z where the remainder of the integrand, $f(k_z)$, is already very small, the integral is small as well. The rapid peaking at high Q plays a crucial role in giving the correct asymptotic behavior of the form factor, as will be discussed in Sec. V B below. Examination of the other propagator in p_+^2 shows a similar behavior, but at negative k_z.

To summarize, for small Q^2, the RIA, by retaining only the spectator pole contribution 1^-, is a good approximation to the CST triangle diagram only for sufficiently large pion masses. For large Q^2, on the other hand, the locations of the poles are insensitive to μ, and therefore the RIA is good not only for large but also for small values of μ (the physical pion mass of $\mu = 0.14$ GeV, for example), and even for vanishing pion mass in the chiral limit. This concludes our discussion of the RIA contribution from the spectator d quark.

Now we turn to the RIA contribution from the diagram where the u quark is the spectator. The locations of the poles can be analyzed in the same way as in the first case; this will not be discussed in detail here. In essence, it is now the positive-energy pole of the spectator u quark (in the lower half k_0 plane) that plays the same role as the spectator pole from the d quark discussed above. This contribution is represented diagrammatically in the lower panel of Fig. 4.

The diagram shown in the lower panel of Fig. 4 can be transformed into the expression for the upper panel, except for a different charge factor. As in the BS case, invariance under the transformation $\hat{k} \to -\hat{k}$, where $\hat{k} = \{E_k, \mathbf{k}\}$ is the on-shell spectator quark momentum, is needed for this transformation, and it is possible because the first
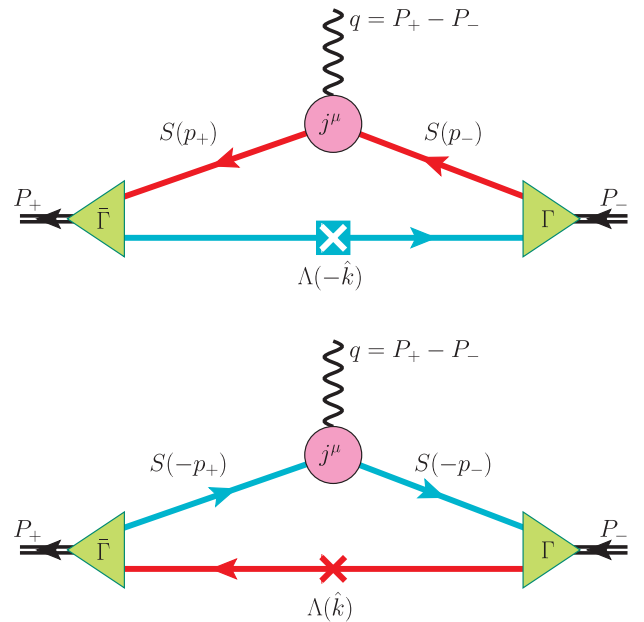

FIG. 4 (color online). The two contributions to the π^+ form factor in the RIA.

contribution is obtained from the *negative-energy* pole contribution of the spectator d quark of the upper half plane and the second from the *positive-energy* pole contribution of the spectator u quark of the lower half plane. The first fixes $k_0 = -E_k$ and the second $k_0 = E_k$, and together with a change of the integration variable $\mathbf{k} \to -\mathbf{k}$ give the symmetry needed to relate the contributions from the u and the d spectators.

Adding the two contributions yields the π^+ form factor in RIA,

$$J^\mu_{\text{RIA}}(P_+, P_-) = e \int_k \text{tr}[\bar{\Gamma}(-\hat{k}, p_+) S(p_+) j^\mu(p_+, p_-)$$
$$\times S(p_-) \Gamma(p_-, -\hat{k}) \Lambda(-\hat{k})]. \quad (9)$$

Here, $p_\pm = P_\pm - \hat{k}$ are the off-shell quark momenta, $\Gamma(p, -\hat{k})$ is the CST pion vertex functions, $\Lambda(\hat{k})$ is the on-shell projector

$$\Lambda(\hat{k}) = \frac{m + \hat{k}}{2m}, \quad (10)$$

and the shorthand

$$\int_k \equiv \int \frac{d^3k}{(2\pi)^3} \frac{m}{E_k} \quad (11)$$

is used for the momentum integration.

IV. INGREDIENTS

In this section, the terms needed for the evaluation of the trace in Eq. (9) are assembled. In the next section, the trace is evaluated and its behavior as $Q \to \infty$ is examined. Numerical results for the form factor are presented in Sec. VI.

A. Pion vertex function

The pion vertex function $\Gamma(p, k)$ is required for the calculation of the trace in Eq. (9). The complete CST pion vertex function is obtained by solving the full four-channel pion bound-state equation of Ref. [1]. This more ambitious task will be the subject of future work. Here we use an approximate pion vertex function that is an *off-shell extension* near the chiral limit. Since the linear confining interaction does not contribute to the pseudoscalar bound-state equation in the chiral limit, as explained in Ref. [1], this estimate will be made using the vector interaction only, with the general form

$$\mathcal{V}_V = \frac{1}{4} V_C \gamma^\mu \otimes \gamma_\mu, \quad (12)$$

where the specific form of the scalar function V_C will be given below. The CST equation for the bound state (but with both external particles off shell) was already derived in Ref. [1]; here we present an alternative derivation starting from the BS bound-state equation written in the rest frame in the chiral limit (where $P = 0$):

$$\Gamma(p, p) = G(p^2)\gamma^5 = i \int_{\text{poles}} \frac{d^4k}{(2\pi)^4} V_C G(k^2) \frac{N}{D}, \quad (13)$$

where $G(p^2)$ is a scalar function, and the notation on the integral reminds us that the k_0 part of the integral is to be evaluated keeping *only* the k_0 poles from the quark propagators (and forsaking all others), and also anticipates the result in the chiral limit, where only the γ^5 structure will contribute to Γ. The numerator in the chiral limit therefore becomes

$$N = \frac{1}{4} \gamma^\mu (M_\chi(k^2) + \not{k}) \gamma^5 (M_\chi(k^2) + \not{k}) \gamma_\mu$$
$$= -(M_\chi^2(k^2) - k^2)\gamma^5, \quad (14)$$

where $M_\chi(k^2)$ is the running mass function in the chiral limit (i.e., with $m_0 = 0$). The denominator is

$$D = (M_\chi^2(k^2) - k^2 - i\epsilon)^2. \quad (15)$$

To obtain the CST equation, we are instructed to take the poles of the propagators *only*, which, after the cancellation of the factor $M_\chi^2(k^2) - k^2$, are single poles at $k_0 = \pm E_k = \pm\sqrt{m_\chi^2 + \mathbf{k}^2}$, with m_χ being the root of the mass equation in the chiral limit, $m_\chi = M_\chi(m_\chi^2)$. Now that one of the initial quarks is on shell, it is possible to specify the scalar function V_C.

As discussed in Ref. [1], in the general case when the total four-momentum P may not be zero,

$$V_C(p_1, p_2; k_1, \hat{k}_2)$$
$$= 2C \frac{E_k}{m} (2\pi)^3 \delta^3(p - k) h(p_1^2) h(p_2^2) h(k_1^2) h(m^2), \quad (16)$$

where $p_1 = p + P/2$, $p_2 = p - P/2$ (and similarly for k_1 and k_2), C is a constant, h is the strong form factor that models the quark-gluon vertex, and in this example $\hat{k}_2^2 = m^2$, with m the dressed quark mass. The chiral limit of Eq. (16) follows by setting $m \to m_\chi$, $P \to 0$, and $h(m_\chi^2) = 1$.

Returning to Eq. (13), extracting the γ^5, and using the chiral limit of Eq. (16) gives

$$G(p^2) = \frac{C}{m_\chi} h^2(p^2) \int d^3k \delta^3(p - k) G(\hat{k}^2)$$
$$= \frac{C}{m_\chi} h^2(p^2) G_0, \quad (17)$$

where $\hat{k} = \{E_k, \mathbf{k}\}$ is the value of the four-vector k at the spectator pole, and the second line employs the definition of the chiral limit of the vertex function, $G(\hat{k}^2) \equiv G_0$. Note that placing the external particle on shell gives a consistent equation only if $C = m_\chi$, which is another way of showing the constraint on C in the chiral limit that was discussed in Ref. [1].

The result in Eq. (17) suggests that near the chiral limit, the vertex functions with one particle on shell should be well approximated by

$$\Gamma(p_1, \hat{p}_2) = \gamma^5 h(p_1^2)G_0, \quad \Gamma(\hat{p}_1, p_2) = \gamma^5 h(p_2^2)G_0. \quad (18)$$

The validity of this approximation depends on the observation that the most rapid variation of the scalar functions that define $\Gamma(p_1, p_2)$ is through its dependence on the strong form factors h.

B. Off-shell quark current

In order to calculate a conserved current for processes involving bound states, we employ the general framework introduced by Riska and Gross [25]. Here the strong form factors (h in this paper) attached to the interaction vertices are moved to the propagators connecting neighboring vertices, where they provide an additional modification of the dressed quark propagators connecting two bare vertices. Consistency then requires that these form factors also be "factored out" of the quark current, leading to the introduction of a *reduced* or *bare* electromagnetic current for the off-shell quarks defined by

$$j_R^\mu(p', p) = h^{-1}(p'^2)j^\mu(p', p)h^{-1}(p^2). \quad (19)$$

In order to ensure current conservation [25,26], j_R^μ must satisfy the Ward-Takahashi (WT) identity:

$$q^\mu j_{R\mu}(p', p) = \tilde{S}^{-1}(p) - \tilde{S}^{-1}(p'), \quad (20)$$

where $\tilde{S}(k)$ is the dressed quark propagator multiplied by the square of the quark form factor

$$\tilde{S}(p) = h^2(p^2)S(p). \quad (21)$$

The simplest form of the reduced current that can satisfy the WT identity [Eq. (20)] with a dressed propagator with a *mass function depending on momentum* is a generalization of the current previously introduced in Ref. [26]:

$$j_R^\mu(p', p) = f(p', p)\left[\mathcal{G}_1^\mu(q) + \kappa F_2(q^2)\frac{i\sigma^{\mu\nu}q_\nu}{2m} \right]$$
$$+ \delta(p', p)\Lambda(-p')\mathcal{G}_4^\mu(q)$$
$$+ \delta(p, p')\mathcal{G}_4^\mu(q)\Lambda(-p)$$
$$+ g(p', p)\Lambda(-p')\mathcal{G}_3^\mu(q)\Lambda(-p), \quad (22)$$

where $\Lambda(-p) = (M(p^2) - \not{p})/2M(p^2)$, and (for $i = 1, 3, 4$),

$$\mathcal{G}_i^\mu(q) \equiv (F_i(q^2) - 1)\tilde{\gamma}^\mu + \gamma^\mu. \quad (23)$$

Here the transverse gamma matrix, $\tilde{\gamma}^\mu = \gamma^\mu - q^\mu\not{q}/q^2$, makes no contribution to the WT identity, and the $F_i(q^2)$ (with $i = 1, \ldots, 4$) are dressed quark form factors (including two new off-shell form factors F_3 and F_4). All of the quark form factors are constrained by $F_i(0) = 1$, with κ being the anomalous magnetic moment of the quark. The functions f, g, and δ are fixed by the requirement that

j_R^μ satisfy the WT identity [Eq. (20)]. Using the notation $h = h(p^2)$, $h' = h(p'^2)$, $M = M(p^2)$, and $M' = M(p'^2)$, with a propagator

$$\tilde{S}^{-1}(p) = \frac{M - \not{p}}{h^2}, \quad (24)$$

a short calculation yields

$$g(p', p) = \frac{4MM'}{h^2h'^2}\frac{h^2 - h'^2}{p'^2 - p^2}, \quad (25)$$

$$\delta(p', p) = \frac{2M'}{h'^2}\frac{M' - M}{p'^2 - p^2}, \quad (26)$$

$$f(p', p) = \frac{M^2 - p^2}{h^2(p'^2 - p^2)} - \frac{M'^2 - p'^2}{h'^2(p'^2 - p^2)}. \quad (27)$$

Note that if $M' = M$, δ vanishes and f and g reduce to results previously given in the literature. When contracted into a conserved current, or a physical photon, the terms proportional to q^μ vanish, reducing $\mathcal{G}_i^\mu(q)$ to

$$\mathcal{G}_i^\mu(q) \rightarrow F_i(q^2)\gamma^\mu. \quad (28)$$

The four quark form factors F_i can be calculated in the CST, but this exercise will be saved for another day. For now we will use the quark current in the chiral limit, where the mass function reduces to [1]

$$M_\chi(p^2) = m_\chi h^2(p^2) \quad (29)$$

and, as appropriate for a pointlike bare quark, $\kappa = 0$ and all form factors are set to unity. This simplifies the off-shell structure functions

$$g_\chi(p', p) = -2\delta_\chi(p', p) = \frac{4m_\chi^2(h^2 - h'^2)}{p'^2 - p^2}, \quad (30)$$

$$f_\chi(p', p) = \frac{1}{4}g_\chi(p', p) + \frac{p'^2h^2 - p^2h'^2}{h^2h'^2(p'^2 - p^2)}$$
$$= \frac{M_\chi^2 - p^2}{h^2(p'^2 - p^2)} - \frac{M_\chi'^2 - p'^2}{h'^2(p'^2 - p^2)} \quad (31)$$

and reduces the current to

$$j_{R_\chi}^\mu(p', p) = \frac{\not{p}'\gamma^\mu\not{p} + p'^2\gamma^\mu}{h'^2(p'^2 - p^2)} - \frac{\not{p}'\gamma^\mu\not{p} + p^2\gamma^\mu}{h^2(p'^2 - p^2)}$$
$$= \gamma^\mu\frac{h^2p'^2 - h'^2p^2}{h^2h'^2(p'^2 - p^2)} + \frac{\not{p}'\gamma^\mu\not{p}}{h^2h'^2}\frac{h^2 - h'^2}{p'^2 - p^2}. \quad (32)$$

It is interesting to compare this with the Ball-Chiu (BC) [27] current used by Maris and Tandy [28]. In our notation, denoting $p' + p = 2P$, their current is

$$j_{BC}^\mu(p', p) = \gamma^\mu\frac{h^2 + h'^2}{2h^2h'^2} + \frac{2\not{P}P^\mu}{h^2h'^2}\frac{h^2 - h'^2}{p'^2 - p^2}. \quad (33)$$

The difference between these two currents is

$$j^\mu_{R_\chi}(p', p) - j^\mu_{BC}(p', p) = \frac{X^\mu}{2h'^2 h^2} \frac{h'^2 - h^2}{p'^2 - p^2}, \quad (34)$$

where X^μ is purely transverse:

$$X^\mu = \not{p}' \gamma^\mu \not{p} = \not{p} \gamma^\mu \not{p}' - \not{q} q^\mu + q^2 \gamma^\mu. \quad (35)$$

The fact that $X^\mu \neq 0$ is a demonstration that the current cannot be uniquely determined by the WT identity alone. It was only after we derived our current that we became aware of the BC current used by Maris and Tandy. In fact, Maris and Tandy used this freedom to add a transverse ρ contribution to their current. In the absence of a dynamical calculation, we know of no way to determine these transverse contributions.

In any case, the quark current can be computed from an integral equation that sums the $q\bar{q}$ interaction to all orders and includes automatically contributions from the $\rho, \rho', \cdots$ tower of vector meson states. Since our formalism can be applied equally well to the timelike region where these states live, this will be explored in the near future.

V. FINAL STEPS

A. Reduction of the current

Substituting Eqs. (18) and (32) into the pion current [Eq. (9)] gives

$$F_\pi(Q^2) 2 P_0^0 = -G_0^2 \int_k \text{tr}[\tilde{S}(p_+) j^0_{R_\chi}(p_+, p_-) \tilde{S}(p_-) \Lambda(\hat{k})], \quad (36)$$

where we keep the pion mass $\mu \neq 0$ but take the chiral limit elsewhere, so that the on-shell quark has mass m_χ (so that E_k is now $\sqrt{m_\chi^2 + \mathbf{k}^2}$), the γ^5's have been removed, and we specialize to the Breit frame [Eq. (5)], where

$$p_\pm^2 = \mu^2 + m_\chi^2 - 2 P_0 E_k \pm k_z Q. \quad (37)$$

Evaluating the trace gives

$$F_\pi(Q^2) = -\frac{G_0^2}{P_0} \int_k \frac{\mathcal{N}}{\mathcal{D}}, \quad (38)$$

where, using the notation $M_\pm = M_\chi(p_\pm^2)$ and $h_\pm = h_\chi(p_\pm^2)$,

$$\begin{aligned}
\mathcal{N} = -2h_\Delta \{ & 4 P_0^2 E_k^3 - 2 P_0 E_k^2 (M_+ M_- + 3\bar{m}^2 - 2 M_S) \\
& + E_k [2\bar{m}^2 (M_+ M_- + \bar{m}^2) - 2 m_\chi M_S (2 P_0^2 + \bar{m}^2) + 4 m_\chi^2 P_0^2 - k_z^2 Q^2 + m_\chi k_z Q M_\Delta] \\
& - m_\chi P_0 [2 m_\chi (M_+ M_- + \bar{m}^2) - 2\bar{m}^2 M_S + k_z Q M_\Delta] \} + 2 k_z Q h_S [m_\chi P_0 (M_S - 2 m_\chi) \\
& + E_k (M_+ M_- + \bar{m}^2 - m_\chi M_S)],
\end{aligned} \quad (39)$$

with $h_S = h_+ + h_-$, $h_\Delta = h_+ - h_-$, $M_S = M_+ + M_-$, $M_\Delta = M_+ - M_-$, and $\bar{m}^2 = m_\chi^2 + \mu^2$. The denominator is

$$\mathcal{D} = 2 k_z Q (M_+^2 - p_+^2)(M_-^2 - p_-^2). \quad (40)$$

To study the convergence of these integrals, look at the limit as k becomes very large (in this section we use the notation $k \equiv |\mathbf{k}|$). In this limit, the running quark masses can be neglected compared to factors of k, giving

$$\begin{aligned}
\mathcal{N} &\xrightarrow{k \gg m_\chi} 2k(h_+^2 - h_-^2)[k_z^2 Q^2 - 4 k^2 P_0^2], \\
\mathcal{D} &\xrightarrow{k \gg m_\chi} 2 k_z Q (4 P_0^2 k^2 - k_z^2 Q^2).
\end{aligned} \quad (41)$$

Ignoring details, the most divergent term therefore behaves like

$$\int_k \frac{\mathcal{N}}{\mathcal{D}} \simeq \int_k h^2, \quad (42)$$

guaranteeing that the integrals will converge if

$$\lim_{k \to \infty} h^2 < \frac{1}{k^2}. \quad (43)$$

This requires that h approach zero faster than k^{-1}.

B. High-Q^2 limit

The high-Q^2 limit of the form factor is particularly interesting. In preparation for this discussion, we use the symmetry of the integrand to convert Eq. (38) to

$$\int_{-\infty}^\infty dk_z \mathcal{F}(k_z) = 2 \int_0^\infty dk_z \mathcal{F}(k_z). \quad (44)$$

Next, we study the arguments p_+^2 and p_-^2 in the limit of large Q. Keeping terms to order $1/Q$ in p_+^2 (which will turn out to be sufficient) gives

$$\begin{aligned}
p_+^2 &\to \mu^2 + m_\chi^2 - Q(E_k - k_z) - \frac{2\mu^2}{Q} E_k, \\
p_-^2 &\to -Q(E_k + k_z).
\end{aligned} \quad (45)$$

Note that as $Q \to \infty$, $p_-^2 \to -\infty$ for all values of k_z, and hence only the leading term is needed. The functions h_- and M_- vanish in that limit. In contrast, the behavior of p_+^2 at large Q depends on the size of k_z. The approximate formula in Eq. (45) shows that $p_+^2 \to -\infty$ at the limits of the k_z integration. We saw already in the discussion of Eq. (8) that the integrand only deviates significantly from zero in the vicinity of the critical value

$$k_{z0} \simeq \frac{QE_\perp}{2\mu}, \tag{46}$$

for which p_+^2 reaches its maximum, and where $E_\perp = (m_\chi^2 + k_\perp^2)^{1/2}$. For large, finite Q, this is a large value of k_z that cannot be ignored. At this critical point,

$$E_k \to \frac{QE_\perp}{2\mu}\left(1 + \frac{2\mu^2}{Q^2}\right), \quad p_+^2 \to p_c^2 = \mu^2 + m_\chi^2 - 2\mu E_\perp. \tag{47}$$

To understand the integral, it is convenient to introduce the momentum fraction

$$x \equiv \frac{E_k - k_z}{2E_k}. \tag{48}$$

The k_z integration will be replaced by an integration over x, and since $k_z > 0$, the x integration varies between 0 and $\frac{1}{2}$, with the Jacobian

$$\int_0^\infty \frac{dk_z}{E_k} = \int_0^{\frac{1}{2}} \frac{dx}{2x(1-x)}. \tag{49}$$

In terms of this variable,

$$E_k = \frac{E_\perp}{2\sqrt{x(1-x)}}, \qquad k_z = \frac{E_\perp(1-2x)}{2\sqrt{x(1-x)}},$$
$$p_+^2 \to \mu^2 + m_\chi^2 - \frac{QE_\perp}{\sqrt{x(1-x)}}\left(x + \frac{\mu^2}{Q^2}\right). \tag{50}$$

The last expression displays clearly how the nonleading term is needed to give the correct limit $p_+^2 \to -\infty$ as $x \to 0$, and that p_+^2 is finite (and hence h_+^2 large) only in the limited region of small $x \sim \mu^2/Q^2$. Hence, we may assume $x \ll 1$ and write

$$p_+^2 \to \mu^2 + m_\chi^2 - \mu E_\perp\left(\sqrt{y} + \frac{1}{\sqrt{y}}\right), \tag{51}$$

with $y = x(Q/\mu)^2$. In terms of the variable y, the integrand peaks near $y \sim 1$, as shown in Fig. 5. Evaluation of the form factor at high Q is therefore ideally suited to a
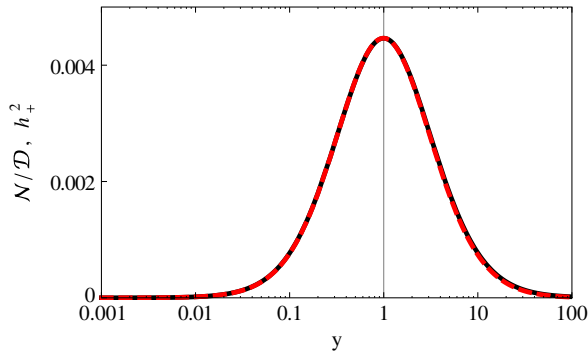

FIG. 5 (color online). $\mathcal{N}/\mathcal{D}$ times a constant (black solid line) compared with h_+^2 (red dashed line) for large Q^2. Both curves lie on top of each other, and they are strongly peaked at $y = 1$.

peaking approximation, with the slowly varying part of the integral evaluated at the peak. Figure 5 compares h_+^2 with the integrand, $\mathcal{N}/\mathcal{D}$, scaled by a constant factor. Both curves lie on top of each other, showing that the peaking approximation works very well. With these approximations, the form factor at large Q becomes

$$F_\pi(Q^2) \overset{Q^2 \gg \mu^2}{\simeq} -\frac{2G_0^2}{Q}\int_{k_\perp}\int_0^\infty \frac{dy}{y}h^2(p_+^2)\left[\frac{\tilde{\mathcal{N}}}{\mathcal{D}}\right]_{\text{peak}}. \tag{52}$$

Evaluation of the terms at the peak gives

$$\tilde{\mathcal{N}} \to -Q^3 \frac{2E_\perp}{\mu^2}[E_\perp^2\mu - 2E_\perp(m_\chi^2 - m_\chi M_+ + \mu^2)$$
$$+ 2m_\chi\mu(m_\chi - M_+)],$$
$$\mathcal{D} \to Q^4 \frac{E_\perp^2}{\mu^2}(M_+^2 - \mu^2 - m_\chi^2 + 2\mu E_\perp). \tag{53}$$

Hence, the form factor falls like Q^{-2} at large Q, with the coefficient independent of the detailed structure of the strong form factor h.

VI. RESULTS

The numerical results for the pion form factor presented in this paper use the simple strong quark form factor $h(p^2)$,

$$h(p^2) = \left(\frac{\Lambda_\chi^2 - m_\chi^2}{\Lambda_\chi^2 - p^2}\right)^n, \tag{54}$$

obtained in Ref. [1]. Here $\Lambda_\chi = 2.04$ GeV is a mass parameter determined by a fit of the quark mass function to the lattice QCD data. The power $n = 2$ is not inconsistent with the lattice data and ensures that the integrals will converge. Note that $h(p^2)$ has a pole at $\Lambda_\chi^2 = p^2$, but this point lies far outside of the region of the k integration.

Our pion form factor is very insensitive to the particular choice of h, as long as $n > 1$ for convergence. This remarkable property can be understood, at least for large Q^2, from the analysis of Sec. V B, which revealed that the high-Q^2 behavior of the form factor integral is completely determined by its integrand evaluated at the peaking value $k_z = k_{z0}$ of h. In this work, we have neglected the anomalous moment term in the quark current, proportional to κ. Conventional arguments suggest that it should be small at large Q and it would vanish for pointlike quarks.

We emphasize that our model, in its present form, gives reliable results only for pion masses in a limited range. In particular, if μ is larger than the threshold value of $\mu_s = 2m_\chi$, the dressed quark propagators develop poles, which allow *both* quarks to go on mass shell *at the same time* [recall the discussion following Eq. (8)]. This can happen only because we have not yet included the confining part of the interaction. Once confinement is included, this cut will vanish. Since the value $\mu_s = 2m_\chi$ is far above the physical pion mass, this does not represent a serious limitation of the present model.

For values of μ below the threshold value $2m_\chi$, we showed in Sec. III that the RIA used in this paper breaks down for small pion masses at small Q^2. This happens because the pole contributions from the struck quark, neglected in RIA, become large. Therefore, the form factor in RIA for a physical pion mass is reasonable at large Q^2, but too large at small Q^2, and does not give the correct charge at $Q^2 = 0$. Therefore, for values of μ somewhere near the chiral quark mass, m_χ, the RIA is a good approximation.

Since the pion form factor depends on the pion mass, we adopt the notation $F_\pi(Q^2, \mu)$. In all cases, $F_\pi(0, \mu) = 1$. We found that the value $\mu = 0.42$ GeV gave the best fit to the data over the full range of Q^2, so we adopted this form factor as a standard of comparison. (Whenever we do not explicitly specify the pion mass in the form factor argument, the value $\mu = 0.42$ GeV is implied.)

We find a remarkable scaling behavior at large Q^2:

$$F_\pi(Q^2, \lambda\mu) \overset{Q^2 \gg \mu^2}{\simeq} \lambda^2 F_\pi(Q^2, \mu), \qquad (55)$$

where λ is a scaling parameter. In particular, Fig. 6 shows the form factor results for $\mu_3 = 0.14$ GeV and

$\mu_2 = 0.28$ GeV when scaled to fit the result for $\mu_1 = 0.42$ GeV. The three curves are compared with the experimental data [29–37].

As Q^2 becomes smaller, the three curves diverge as a consequence of the breakdown of the RIA in the small-Q^2 region for small μ. In the high-Q^2 region, as shown in the top panel of Fig. 7, the curves almost lie on top of each other. Furthermore, if the Q^2 dependence is also scaled over the whole range of Q^2,

$$F_\pi(\lambda^2 Q^2, \lambda\mu) \simeq F_\pi(Q^2, \mu), \qquad (56)$$

the curves almost lie on top of each other, even at small Q^2. This expresses the fact that our form factor depends very weakly on the remaining scale-dependent quantities, m_χ and Λ_χ.

The form factors satisfy a nearly monopole behavior

$$F_\pi(Q^2) \overset{Q^2 \gg \mu^2}{\sim} \frac{1}{Q^2 + \nu^2}, \qquad (57)$$

with a mass scale of $\nu \simeq 0.63$ GeV obtained from a fit to the $\mu_1 = 0.42$ GeV form factor.
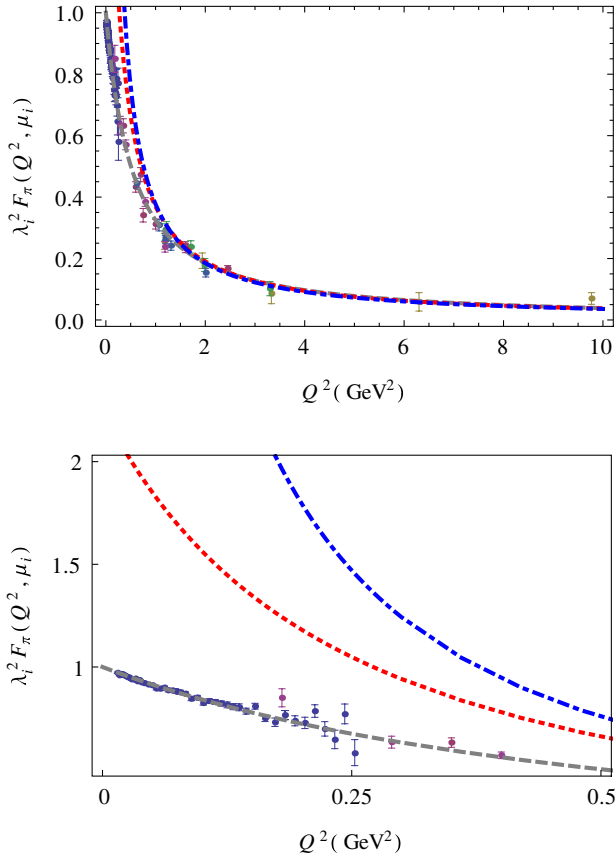

FIG. 6 (color online). The pion form factor $F_\pi(Q^2, \mu_i)$ scaled with $\lambda_i^2 = (\mu_1/\mu_i)^2$ for different pion masses $\mu_1 = 0.42$ GeV (gray dashed line), $\mu_2 = 0.28$ GeV (red dotted line) and $\mu_3 = 0.14$ GeV (blue dot-dashed line), compared with the data [29–37] at high Q^2 (top) and low Q^2 (bottom).
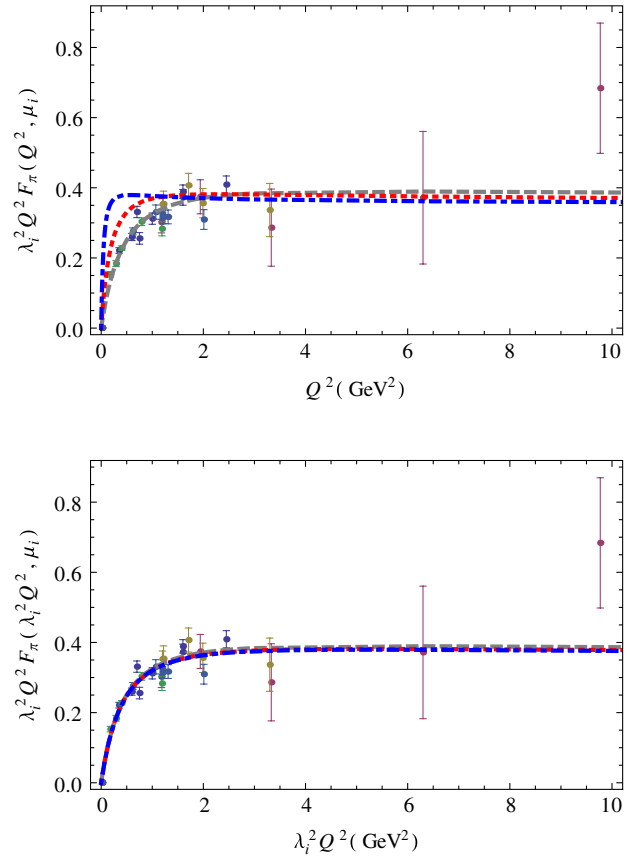

FIG. 7 (color online). Scaled form factors compared to the data [29–37]. The top panel shows $\lambda_i^2 Q^2 F_\pi(Q^2, \mu_i)$; the bottom shows $\lambda_i^2 Q^2 F_\pi(\lambda_i^2 Q^2, \mu_i)$. In both panels, $\lambda_i = \mu_1/\mu_i$ for different pion masses $\mu_1 = 0.42$ GeV (gray dashed line), $\mu_2 = 0.28$ GeV (red dotted line) and $\mu_3 = 0.14$ GeV (blue dot-dashed line).

VII. SUMMARY AND CONCLUSIONS

This paper uses the covariant spectator theory (CST) to compute the pion form factor in the relativistic impulse approximation (RIA). The CST is formulated in Minkowski space, so that even though results for the form factor at spacelike momentum transfer ($q^2 = -Q^2 < 0$) are presented here, the theory can be used to calculate the form factor in the timelike region ($q^2 > 0$) as well. The manifestly covariant dynamical model for the $q\bar{q}$ interaction that is the foundation of the calculations presented here incorporates both spontaneous chiral symmetry breaking and confinement, and it is discussed in Ref. [1]. Some features of these models were previously introduced by Gross, Milana and Şavkli [38,39].

This first calculation of the pion form factor uses the quark mass function obtained in Ref. [1] and expresses the pion vertex function in terms of this mass function. This approximation is particularly good near the chiral limit. We emphasize that this is a very simple picture for the pion. Still, when combined with the results of Ref. [1], we show that this simple picture can give results that are in good agreement with both the lattice data for the dressed quark mass and the experimental data for the pion electromagnetic form factor. We find some interesting scaling relations relating form factors with different values of μ.

An interesting issue remains. This simple model is able to describe the data well, yet it seems to include no contribution from the ρ meson that is expected from vector meson dominance. (For a comparison of our model with what is expected from a simple ρ pole, see Fig. 8.) Where is the ρ contribution? It should be contained in the dressing of the quark current, j^μ. Maris and Tandy [28] suggest that their Ball-Chiu current contains some of these contributions (in which case our dressed current probably also contains them). The balance between the triangle diagram with no ρ contribution and contributions coming from the
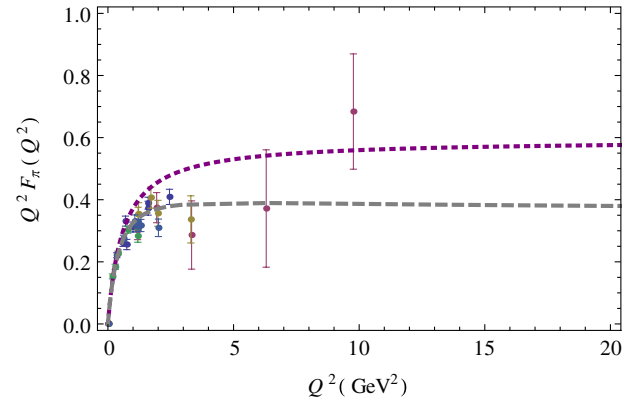

FIG. 8 (color online). A ρ-pole contribution to the pion form factor, normalized to unity at $Q^2 = 0$ (purple dotted line), compared to our calculation with $\mu = 0.42$ GeV (gray dashed line).

dynamical dressing of the quark current, including the ρ pole, will best be understood once the dressed quark current has been calculated in both the timelike and spacelike regions.

For a more quantitative study of the light meson properties, the solution of the complete four-channel CST equation and a fit to the light meson spectrum is needed, which will be the subject of our future program.

[1] E. P. Biernat, F. Gross, M. T. Pena, and A. Stadler, preceding article, Phys. Rev. D **89**, 016005 (2014).

[2] F. Gross, Phys. Rev. **186**, 1448 (1969).

[3] F. Gross, Phys. Rev. D **10**, 223 (1974).

[4] F. Gross, Phys. Rev. C **26**, 2203 (1982).

[5] F. Gross, G. Ramalho, and M. T. Pena, Phys. Rev. C **77**, 015202 (2008).

[6] S. A. Pinto, A. Stadler, and F. Gross, Phys. Rev. C **79**, 054006 (2009).

[7] P. Maris and P. C. Tandy, Phys. Rev. C **61**, 045202 (2000).

[8] L. Chang, I. Cloet, C. Roberts, S. Schmidt, and P. Tandy, Phys. Rev. Lett. **111**, 141802 (2013).

[9] F. Coester and W. N. Polyzou, Phys. Rev. C **71**, 028202 (2005).

[10] S. J. Brodsky and G. F. de Teramond, Phys. Rev. D **77**, 056007 (2008).

[11] J. P. B. C. de Melo, T. Frederico, E. Pace, and G. Salme, Phys. Rev. D **73**, 074013 (2006).

[12] J. Carbonell, V. Karmanov, and M. Mangin-Brinet, Eur. Phys. J. A **39**, 53 (2009).

[13] E. P. Biernat, W. Schweiger, K. Fuchsberger, and W. H. Klink, Phys. Rev. C **79**, 055203 (2009).

[14] D. Ebert, R. Faustov, and V. Galkin, Eur. Phys. J. C **47**, 745 (2006).

[15] P. Masjuan, S. Peris, and J. J. Sanz-Cillero, Phys. Rev. D **78**, 074028 (2008).

[16] B. Ananthanarayan, I. Caprini, and I. S. Imsong, Phys. Rev. D **85**, 096006 (2012).

[17] B. Ananthanarayan, I. Caprini, D. Das, and I. Sentitemsu Imsong, Eur. Phys. J. C **72**, 2192 (2012).
[18] B. Ananthanarayan, I. Caprini, D. Das, and I. Sentitemsu Imsong, Eur. Phys. J. C **73**, 2520 (2013).
[19] S. V. Troitsky and V. E. Troitsky, Phys. Rev. D **88**, 093005 (2013).
[20] F. Gross and B. D. Keister, Phys. Rev. C **28**, 823 (1983).
[21] F. Gross, Phys. Rev. **140**, B410 (1965).
[22] R. G. Arnold, C. E. Carlson, and F. Gross, Phys. Rev. Lett. **38**, 1516 (1977).
[23] R. G. Arnold, C. E. Carlson, and F. Gross, Phys. Rev. C **21**, 1426 (1980).
[24] J. W. Van Orden, N. Devine, and F. Gross, Phys. Rev. Lett. **75**, 4369 (1995).
[25] F. Gross and D. O. Riska, Phys. Rev. C **36**, 1928 (1987).
[26] Y. Surya and F. Gross, Phys. Rev. C **53**, 2422 (1996).
[27] J. S. Ball and T. W. Chiu, Phys. Rev. D **22**, 2542 (1980).

[28] P. Maris and P. C. Tandy, Phys. Rev. C **61**, 045202 (2000).
[29] S. Amendolia *et al.*, Nucl. Phys. **B277**, 168 (1986).
[30] C. Brown, C. Canizares, W. Cooper, A. Eisner, G. Feldman, C. Lichtenstein, L. Litt, W. Lockeretz, V. Montana, and F. Pipkin, Phys. Rev. D **8**, 92 (1973).
[31] C. J. Bebek *et al.*, Phys. Rev. D **9**, 1229 (1974).
[32] C. Bebek, C. Brown, M. Herzlinger, S. Holmes, C. Lichtenstein, F. Pipkin, S. Raither, and L. Sisterson, Phys. Rev. D **13**, 25 (1976).
[33] C. J. Bebek *et al.*, Phys. Rev. D **17**, 1693 (1978).
[34] J. Volmer *et al.*, Phys. Rev. Lett. **86**, 1713 (2001).
[35] T. Horn *et al.*, Phys. Rev. Lett. **97**, 192001 (2006).
[36] V. Tadevosyan *et al.*, Phys. Rev. C **75**, 055205 (2007).
[37] G. M. Huber *et al.*, Phys. Rev. C **78**, 045203 (2008).
[38] F. Gross and J. Milana, Phys. Rev. D **43**, 2401 (1991); **45**, 969 (1992); **50**, 3332 (1994).
[39] C. Savkli and F. Gross, Phys. Rev. C **63**, 035208 (2001).